

# Experimental Observation of Information Flow in the Anti- $\mathcal{PT}$ -Symmetric System

Jingwei Wen<sup>1</sup>, Guoqing Qin<sup>1</sup>, Chao Zheng<sup>4</sup>, Shijie Wei<sup>1,5</sup>, Xiangyu Kong<sup>1</sup>, Tao Xin<sup>6,7,8</sup>,\* and Guilu Long<sup>1,2,3†</sup>

<sup>1</sup> State Key Laboratory of Low-Dimensional Quantum Physics and  
Department of Physics, Tsinghua University, Beijing 100084, China

<sup>2</sup> Tsinghua National Laboratory for Information Science and Technology, Beijing 100084, P. R. China

<sup>3</sup> Collaborative Innovation Center of Quantum Matter, Beijing 100084, China

<sup>4</sup> Department of Physics, College of Science, North China University of Technology, Beijing 100144, China

<sup>5</sup> Beijing Academy of Quantum Information Sciences, Beijing 100193, China

<sup>6</sup> Shenzhen Institute for Quantum Science and Engineering,

Southern University of Science and Technology, Shenzhen 518055, China

<sup>7</sup> Center for Quantum Computing, Peng Cheng Laboratory, Shenzhen 518055, China and

<sup>8</sup> Shenzhen Key Laboratory of Quantum Science and Engineering,

Southern University of Science and Technology, Shenzhen 518055, China

The recently theoretical and experimental researches related to  $\mathcal{PT}$ -symmetric system have attracted unprecedented attention because of various novel features and potentials in extending canonical quantum mechanics. However, as the counterpart of  $\mathcal{PT}$ -symmetry, there are only a few researches on anti- $\mathcal{PT}$ -symmetry. Here, we propose an algorithm for simulating the universal anti- $\mathcal{PT}$ -symmetric system with quantum circuit. Utilizing the protocols, an oscillation of information flow is observed for the first time in our Nuclear Magnetic Resonance quantum simulator. We will show that information will recover from the environment completely when the anti- $\mathcal{PT}$ -symmetry is broken, whereas no information can be retrieved in the symmetry-unbroken phase. Our work opens the gate for practical quantum simulation and experimental investigation of universal anti- $\mathcal{PT}$ -symmetric system in quantum computer.

Traditional quantum mechanics requires Hermitian Hamiltonians to describe closed physical systems, while the dynamic evolution of open systems is typically described by non-Hermitian Hamiltonians [1, 2]. The non-hermitian Hamiltonian of open systems has attracted extensive attention and research because of the discovery by Bender and Boettcher in 1998 [3]. It was found that Hamiltonians satisfying parity  $\mathcal{P}$  (spatial reflection) and  $\mathcal{T}$  (time reversal) symmetry instead of hermiticity can still have real energy spectra and orthogonal eigenstates in the symmetry-unbroken phase, in which the eigenfunction of system Hamiltonian is at the same time an eigenfunction of the  $\mathcal{PT}$  operator [4, 5]. When the Hamiltonian parameters cross the exceptional point,  $\mathcal{PT}$ -symmetry will be broken and lead to a symmetry-breaking transition [6–8]. This work has inspired numerous theoretical and experimental studies [9–15] of the non-hermitian systems, including demonstrating novel properties of open systems [16, 17] and extending fundamental quantum mechanics [20, 21]. However, there are limited investigations on another important counterpart anti- $\mathcal{PT}$ -symmetry, which means the system Hamiltonian is anti-commutative with the joint  $\mathcal{PT}$  operator  $\{H, \mathcal{PT}\} = 0$ . Some relevant experimental demonstrations have been realized in atoms [29–31], optical [32–37], electrical circuit resonators [38] and diffusive systems [39]. Quantum processes such as symmetry breaking transition, observation of exceptional point and simulation of anti- $\mathcal{PT}$ -symmetric Lorentz dynamics have been presented in these experiments [29, 33, 37, 38], whereas the novel characteristics of entanglement [17–19] and information flow [22–24] in the anti- $\mathcal{PT}$ -symmetric system,

which would present various phenomena different from Hermitian quantum mechanics and reveal the relationship between system and environment, have not been fully thorough investigated in the experiment.

In this work, we propose an algorithm for the simulation of universal anti- $\mathcal{PT}$ -symmetric evolution with quantum circuit model and report the first experimental observation of information flow oscillation in anti- $\mathcal{PT}$ -symmetric system on Nuclear Magnetic Resonance quantum computing platform. It is based on decomposing the non-Hermitian Hamiltonian evolution into a sum of unitary operators and realizing the simulation in an enlarged Hilbert space with ancillary qubits [40]. We will show that the information flow oscillates back and forth between the environments and system in broken phase and the phenomenon of information backflow occurs, which means that information flows from the environment back to the system and this does not happen in traditional Hermitian quantum mechanics [22, 25, 26]. The oscillation period and amplitude increase as the system parameters approach the exceptional point. When passing through the critical point, the information backflow no longer occurs, and can only be attenuated exponentially from the system and leakage information into the environment. The monotone correspondence relation can provide a way to measure the degree of hermiticity for an open system. The phase-breaking and information flow transition at exceptional point observed in our experiment also mean the transition from non-Markovian process to Markovian process [24, 27, 28].

*Construction of simulation scheme*—For an arbitrary  $n$ -dimensional target evolution operator, it can always

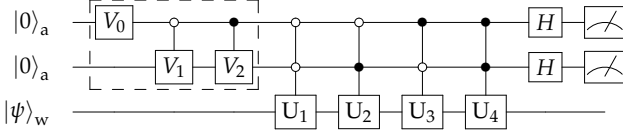


FIG. 1: Quantum circuits for the simulation of universal anti- $\mathcal{PT}$ -symmetric single-qubit system. Single-qubit operators  $V_0$  and  $H$  (Hadamard gate) are operated on the ancillary qubits and two two-qubit operators (0-controlled  $V_1$  and 1-controlled  $V_2$ ) are implemented to the system followed by four three-qubit controlled quantum gates  $U_i (i \in (1, 2, 3, 4))$  and we achieve anti- $\mathcal{PT}$ -symmetric evolution on the work qubit by collapsing the ancillary qubits into  $|00\rangle\langle 00|$  based on our parameters setup.

be decomposed into the form  $U = \sum_{i=1}^d \alpha_i U_i$  and coefficients  $\alpha_i$  depend on the choice of decomposition but satisfy construction condition  $\sum_{i=1}^d |\alpha_i| = \alpha$ . Then, by constructing operators  $\hat{G} = \sum_{i=1}^d \sqrt{\frac{\alpha_i}{\alpha}} |i\rangle\langle 0|$  working on the ancillary qubits and controlled-operator  $\hat{U} = \sum_{i=1}^d |i\rangle\langle i| \otimes U_i$ , we can realize the simulation of Hamiltonian evolution in the subspace of  $\langle 0|\hat{G}^\dagger \hat{U} \hat{G}|0\rangle$  [40–43]. For a single-qubit system, the universal form of anti- $\mathcal{PT}$ -symmetric Hamiltonian can be written as

$$\hat{H}_{\mathcal{AP}\mathcal{T}} = \begin{pmatrix} re^{i\theta} & is \\ i\mu & -re^{-i\theta} \end{pmatrix} \quad (1)$$

where all the parameters  $r, \theta, s, \mu$  are real numbers. Unlike  $\mathcal{PT}$ -symmetry which means system Hamiltonian  $\hat{H}_{\mathcal{PT}}$  commutes with joint operator  $\mathcal{PT}$ , anti- $\mathcal{PT}$ -symmetric Hamiltonian satisfies anti-commutation relation  $\mathcal{P}\hat{H}_{\mathcal{AP}\mathcal{T}}\mathcal{P} = -\hat{H}_{\mathcal{AP}\mathcal{T}}$ , where operator  $\mathcal{P}$  is the Pauli  $\sigma_x$  matrix and the time-reversal operator  $\mathcal{T}$  corresponds to complex conjugation. The eigenvalues of Hamiltonian  $\hat{H}_{\mathcal{AP}\mathcal{T}}$  are  $\varepsilon_{\pm} = ir \sin \theta \pm \sqrt{r^2 \cos^2 \theta - \mu s}$  and the system is termed in the regime of unbroken anti- $\mathcal{PT}$ -symmetric phase when  $r^2 \cos^2 \theta - \mu s < 0$ . For convenience, we set the difference between the two eigenvalues as  $w = \varepsilon_+ - \varepsilon_- = 2\sqrt{r^2 \cos^2 \theta - \mu s}$ . The dynamics governed by an anti- $\mathcal{PT}$ -symmetric non-Hermitian Hamiltonian  $\hat{H}_{\mathcal{AP}\mathcal{T}}$  is described by

$$\hat{\rho}(t) = \frac{e^{-i\hat{H}_{\mathcal{AP}\mathcal{T}}t} \hat{\rho}(0) e^{i\hat{H}_{\mathcal{AP}\mathcal{T}}t}}{\text{tr}[e^{-i\hat{H}_{\mathcal{AP}\mathcal{T}}t} \hat{\rho}(0) e^{i\hat{H}_{\mathcal{AP}\mathcal{T}}t}]} \quad (2)$$

Here we employ the usual Hilbert-Schmidt inner product instead of a preferentially selected one and consider the effective non-unitary dynamics of an open quantum system [22, 44]. We construct a general single-qubit anti- $\mathcal{PT}$  symmetric quantum system to simulate the dynamics evolution in Eq.(2) by enlarging the system with entangled ancillary qubits and encoding the subsystem with the non-Hermitian Hamiltonian with post-selection.

Quantum circuit used to simulate the anti- $\mathcal{PT}$ -symmetric evolution is shown in Fig.(1) including two

ancillary qubits and one work qubit forming a three-qubit scheme. The initial state is prepared in  $|00\rangle_a |\psi\rangle_w$  first, then an unitary operator  $V_0$  and two two-qubit operators (0-controlled  $V_1$  and 1-controlled  $V_2$ ) are implemented on the ancillary qubits just as shown in the dotted box. The operation in the dotted box is equivalent to an operator  $V$  and only the first column is definable. The first column of two-qubit operator  $V$  without considering the normalization constant is  $[V_{11}, V_{21}, V_{31}, V_{41}]$  and

$$\begin{aligned} V_{11} &= \cos(wt/2\hbar), & V_{21} &= \frac{s + \mu}{w} \sin(wt/2\hbar) \\ V_{31} &= i \frac{s - \mu}{w} \sin(wt/2\hbar), & V_{41} &= \frac{-2ir \cos \theta}{w} \sin(wt/2\hbar) \end{aligned} \quad (3)$$

It does not matter what the other matrix elements in operator  $V$  are, while we can determine the operator by Schmidt Orthogonalization under the constrain that the operator must be unitary. We can also decompose it into single and two-qubit operators just as shown in the dotted box of Fig.(1). Suppose that the normalized first column of the two-qubit operator is  $[V'_{11}, V'_{21}, V'_{31}, V'_{41}]$  satisfying normalization conditions  $\sum_{i=1}^4 |V'_{i1}|^2 = 1$ , and then we can construct  $4 \times 4$  unitary matrix  $V$  that satisfies the constrain and the concrete form of operators can be determined by Eq.(4).

$$V = (V_1 \oplus V_2) \cdot (V_0 \otimes I) \quad (4)$$

where the single-qubit unitary operators  $V_0$  and two-qubit controlled operators  $V_k (k = 1, 2)$  are determined by

$$\begin{aligned} V_0 &= \begin{pmatrix} \sqrt{|V'_{11}|^2 + |V'_{21}|^2} & \sqrt{|V'_{31}|^2 + |V'_{41}|^2} \\ \sqrt{|V'_{31}|^2 + |V'_{41}|^2} & -\sqrt{|V'_{11}|^2 + |V'_{21}|^2} \end{pmatrix} = R(\theta_0) \\ V_k &= \begin{pmatrix} V'_{2k-1,1} & V'_{2k,1} \\ \sqrt{|V'_{2k-1,1}|^2 + |V'_{2k,1}|^2} & \sqrt{|V'_{2k-1,1}|^2 + |V'_{2k,1}|^2} \\ V'_{2k,1} & -V'_{2k-1,1} \\ \sqrt{|V'_{2k-1,1}|^2 + |V'_{2k,1}|^2} & \sqrt{|V'_{2k-1,1}|^2 + |V'_{2k,1}|^2} \end{pmatrix} = R(\theta_k) \end{aligned} \quad (5)$$

The rotation operator can be expressed as  $R(\theta_l) = \begin{pmatrix} \cos \theta_l & \sin \theta_l \\ \sin \theta_l & -\cos \theta_l \end{pmatrix}$ , ( $l = 0, 1, 2$ ). According to the decomposition method and parameters in the anti- $\mathcal{PT}$ -symmetric Hamiltonian, we can determine the explicit forms of the angles in the three operators.

$$\begin{aligned} \theta_0 &= \arccos \sqrt{\frac{w^2 \cos^2(wt/2\hbar) + (\mu + s)^2 \sin^2(wt/2\hbar)}{w^2 + 2(\mu + s)^2 \sin^2(wt/2\hbar)}} \\ \theta_1 &= \arccos \frac{w \cos(wt/2\hbar)}{\sqrt{w^2 \cos^2(wt/2\hbar) + (\mu + s)^2 \sin^2(wt/2\hbar)}} \\ \theta_2 &= \arccos \frac{i(s - \mu)}{\sqrt{(\mu - s)^2 + 4r^2 \cos^2 \theta}} \end{aligned} \quad (6)$$

The single-qubit operator  $V_0$  and two controlled- $V_k (k = 1, 2)$  gates are all unitary, which is feasible to realize in quantum computation frame. Next, the three-qubit controlled- $U_i (i = 1, 2, 3, 4)$  construct a set of complete basis in two-dimensional Hilbert space on the work

system, which means operators  $U_i$  can be set as identity matrix  $\sigma_0 = I_{2 \times 2}$  and Pauli matrix  $\sigma_x, \sigma_y, \sigma_z$ . Finally, two Hadamard gates are applied on the ancillary qubits to mix up the states and the target quantum state  $\hat{\rho}(t)$  of the work system can be obtained when two ancillary qubits collapse into state  $|00\rangle\langle 00|$  according to our parameters setup. It is worth emphasizing that our scheme works for both unbroken and broken anti- $\mathcal{PT}$ -symmetric phase, even at the exceptional point. Therefore, our protocol provides a novel method to investigate various properties of anti- $\mathcal{PT}$ -symmetric system.

*Experimental Application*—To present the information retrieval in anti- $\mathcal{PT}$ -symmetric system, we identify the information flow by trace distance between two quantum states  $D(\hat{\rho}_1(t), \hat{\rho}_2(t)) = \frac{1}{2} \text{tr}|\hat{\rho}_1(t) - \hat{\rho}_2(t)|$  and  $|\hat{M}| = \sqrt{\hat{M}^\dagger \hat{M}}$ . The trace distance keeps invariant under unitary transformations whereas does not increase under completely positive and trace-preserving maps which means the unidirectional information flow from the system to environment will not be recovered. However, the complete information retrieval from the environment in  $\mathcal{PT}$ -symmetric system has been proposed in theory [22]. In contrast, there has been little research in the counterpart anti- $\mathcal{PT}$ -symmetric system and in this work, we observed an oscillation of information flow in anti- $\mathcal{PT}$ -symmetric single-qubit system in experiment based on our Nuclear Magnetic Resonance platform.

As a proof-of-principle experiment, we consider a two-level anti- $\mathcal{PT}$ -symmetric system  $H_{APT} = s(i\hat{\sigma}_x + \lambda\hat{\sigma}_z)$ , where  $s \geq 0$  is an energy scale and  $\lambda \geq 0$  is a coefficient representing the degree of Hermiticity. The eigenvalues of the Hamiltonian are  $\pm s\sqrt{\lambda^2 - 1}$  and the anti- $\mathcal{PT}$ -symmetry will be unbroken if  $\lambda < 1$  and the two-order exceptional point is located at  $\lambda = 1$ . The dynamic evolution under  $H_{APT}$  can be realized via our protocol presented above by setting the parameters in Eq.(1) as  $\theta = 0$  and  $r = \lambda s = \lambda\mu$  appropriately. We take different  $\lambda$  values in both anti- $\mathcal{PT}$ -symmetric unbroken and broken region to observe the dynamic feature of the system. We need to evolve the system under anti- $\mathcal{PT}$ -symmetric dynamics with different initial state  $|0\rangle\langle 0|$  and  $|1\rangle\langle 1|$  to determine the distinguishability and we extend the controlled gates  $U_i = \sigma_i$  to two-qubit Hilbert space  $U_i = \sigma_i \otimes \sigma_i$  ( $i \in \{0, x, y, z\}$ ) and add one more rotation  $\sigma_x$  on the second work qubit. Therefore, the quantum systems in two different Hilbert space undergo the same dynamics evolution induced by anti- $\mathcal{PT}$ -symmetric Hamiltonian only with different initial state and by this experimental setup, we can reduce the random error caused by the change of environment.

In experiments, we use the spatial averaging technique to prepare the pseudo-pure state [45, 46] from the thermal equilibrium with  $^{13}\text{C}$ -labeled transcrotonic acid dissolved in d6-acetone as the four-qubit sample. The internal Hamiltonian under weak coupling approximation

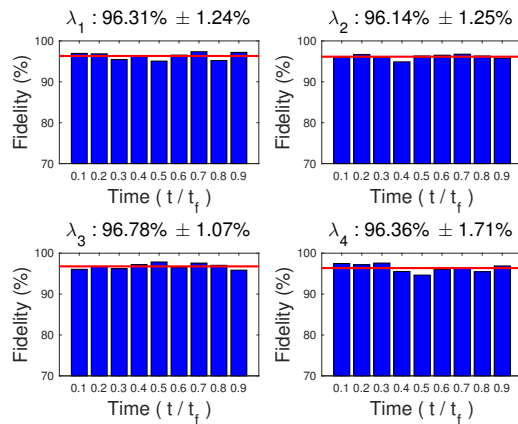


FIG. 2: Fidelities between the experimental results and theoretical expectation. The average fidelities labelled by red lines are over 96% and the maximum deviations are within 2%.

is  $H_{int} = -\sum_{i=1}^4 \pi\nu_i\sigma_z^i + \sum_{i<j}^4 \frac{\pi}{2} J_{ij}\sigma_z^i\sigma_z^j$ , where  $\nu_i$  is the chemical shift and  $J_{ij}$  is the J-coupling strength between the  $i$ th and  $j$ th nuclei. All the parameters are determined by experimental measurement and the form of the initial state is  $|\rho_{0000}\rangle = (1 - \epsilon)I/16 + \epsilon|0000\rangle\langle 0000|$  and  $\epsilon \approx 10^{-5}$  is the polarization. The first item doesn't evolve under unitary operators and the second deviated part is equivalent to quantum pure state. The fidelities between experimental and ideal pure state  $|0000\rangle$  are over 99.5%, which are calculated by the definition  $F(\rho, \sigma) = \text{tr}(\rho\sigma) / \sqrt{\text{tr}\rho^2} \sqrt{\text{tr}\sigma^2}$  [51]. Subsequently, we apply the quantum operations in our algorithm according to the different parameter setup. We fix evolution time  $t_f = 1\text{s}$  and set  $s = 3$  as the energy scale. Four values of  $\lambda \in \{2, 1.5, 1.01, 0.5\}$  are chosen and the former three are located at broken phase and the last one leads to unbroken anti- $\mathcal{PT}$ -symmetry. All the operations are realized using shaped pulses optimized by the gradient method [47]. Each shaped pulse is simulated to be over 99.5% fidelity while being robust to the static field distributions and inhomogeneity. By performing four-qubit quantum state tomography [48–50], we obtain the target density matrix when the ancillary qubits are  $|00\rangle$  at the end of circuit. We extract nine discrete time points and the mean fidelities between the theoretical expectations and experimental values are over 96% in Fig.(2). The information flow identified by experimental results are plotted in Fig.(3). Because of the random fluctuations of the amplitude and phase in control field, the experimental results produce some random errors. We suppose that the random fluctuations are within a range of 5% in amplitude and in phase, which are common in actual experimental process, then the fluctuation range of distinguishability are also plotted as the errorbar.

*Analysis of experimental results*—Our experimental results clearly show that the distinguishability oscillates

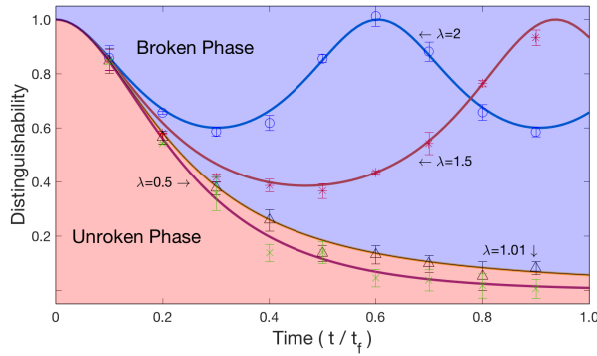


FIG. 3: Experimental results of information flow measured by distinguishability. Four  $\lambda$  values are set in our experiment including three broken anti- $\mathcal{PT}$ -symmetric phase and one unbroken point. The solid lines represent theoretical values, and the nine discrete points on each line are experimental results. Theoretical error range of distinguishability are numerically analyzed based on the assumption that fluctuations of amplitude and phase are within a range of 5%.

with evolution time when the system symmetry is broken and information can retrieve from the environment completely. The closer you get to the exceptional point, the bigger the period gets and the larger the amplitude of information vibration becomes, which means the system undergoes larger fluctuations. However, the distinguishability decays with time and no information recover from the environment in the unbroken anti- $\mathcal{PT}$ -symmetric phase. The distinguishability oscillates with period  $T = \pi\hbar/(s\sqrt{\lambda^2 - 1})$  and in order to validate our experimental results about change trend, we theoretically analyze the oscillation period and amplitude just as shown in Fig.(4). Such a change trend means that if  $\lambda$  is large enough, the distinguishability will maintain unchanged at value one, which corresponds to the physical explanation that the non-Hermitian part ( $i\hat{\sigma}_x$ ) in system Hamiltonian can be ignored compared with the Hermitian part ( $\lambda\hat{\sigma}_z$ ). Then the evolution process of the system can be approximate to unitary evolution, in which the information flow does not oscillate. In the symmetry-unbroken phase, the amplitude keeps value one and the period is zero, which means the system will lose all the information into the environment and information back-flow does not occur. Therefore, the behavior of the system can be consistently understood and interpreted, whether it is an Hermitian or an anti- $\mathcal{PT}$ -symmetric system. In addition, the increase of distinguishability in the broken phase implies that the anti- $\mathcal{PT}$ -symmetric system exhibits unique non-Markovian behavior as well [22, 23]. To further determine the evolution characteristics, we theoretically calculated the purity of the quantum state in Fig.(5) and observed similar oscillation and attenuation phenomena just like information flow. This means that the quantum state evolving under the anti-

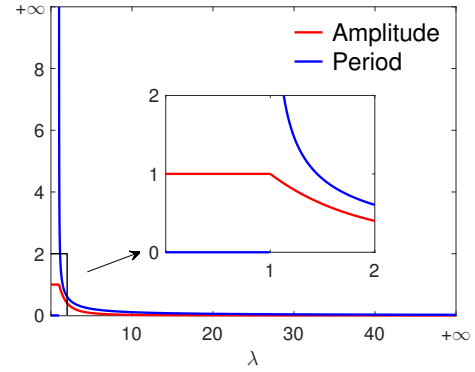


FIG. 4: The amplitude and period of distinguishability as functions of  $\lambda$  according the same parameter setup in experiment. The locally enlarged subgraph is the change trend around exceptional point.

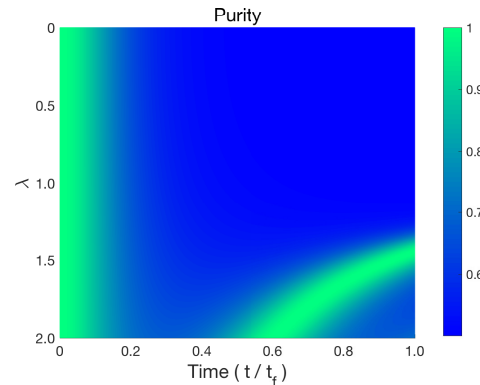


FIG. 5: Purity of quantum state evolving with time under different  $\lambda$  values. When parameters locate in the unbroken anti- $\mathcal{PT}$ -symmetric phase ( $\lambda < 1$ ), purity will decay exponentially with time and approach value 0.5, which means a maximum mixed state. The oscillation of purity can be observed in the broken phase.

$\mathcal{PT}$ -symmetric Hamiltonian will be entangled with the environment so as to a decoherence process, but the process is reversible in the case of broken phase and irreversible in the unbroken phase.

*Conclusion*—We propose an algorithm for the simulation of universal anti- $\mathcal{PT}$ -symmetric system and observe an oscillation of information flow in experiment. We compare the performance when system parameters approach exceptional point and change from anti- $\mathcal{PT}$ -symmetric broken phase into unbroken phase. It is found that both the oscillation period and amplitude increase monotonically before the phase transition, whereas no information will be retrieved from the environment any more after passing the critical point, which means that we have also realized a symmetry breaking process in anti- $\mathcal{PT}$ -symmetric system. The monotone correspondence relation in symmetry-broken phase implies that

our results could supply a metric method to measure the degree of non-hermiticity ( $\propto$  amplitude  $\in (0, 1)$ ) for an open system. The change tendency of the information flow obtained in our experiment could supply a consistent understanding method for the Hermitian and anti- $\mathcal{PT}$ -symmetric systems. Our proposed scheme can be extended to high-dimensional cases and other quantum computing platforms.

This work was supported by the National Basic Research Program of China under Grant Nos.2017YFA0303700 and 2015CB921001, National Natural Science Foundation of China under Grant Nos.61726801, 11474168 and 11474181. C. Z is supported by National Natural Science Foundation of China Grant No. 11705004, Open Research Fund Program of the State Key Laboratory of Low-Dimensional Quantum Physics No. KF201710. T. X is also supported by the Science, Technology and Innovation Commission of Shenzhen Municipality (No. ZDSYS20170303165926217, No. JCYJ20170412152620376) and Guangdong Innovative and Entrepreneurial Research Team Program (Grant No. 2016ZT06D348).

---

\* Electronic address: [xint@sustech.edu.cn](mailto:xint@sustech.edu.cn)

† Electronic address: [gllong@tsinghua.edu.cn](mailto:gllong@tsinghua.edu.cn)

- [1] J. von Neumann, *Math. Ann.* **102**, 49 (1930).
- [2] Ángel Rivas and Susana F. Huelga, *arXiv*. **1104**, 5242 (2012).
- [3] Carl M. Bender and Stefan Boettcher, *Phys. Rev. Lett.* **80**, 5243 (1998).
- [4] Vladimir V. Konotop, Jianke Yang, and Dmitry A. Zezyulin, *Rev. Mod. Phys.* **88**, 035002 (2016).
- [5] Ramy El-Ganainy *et al.*, *Nature Physics*. **14**, 11-19 (2018).
- [6] Thomas J. Milburn *et al.*, *Phys. Rev. A*. **92**, 052124 (2015).
- [7] Dieter Heiss, *Nature Physics*. **12**, 823-824 (2016).
- [8] Carl M. Bender *et al.*, *Phys. Rev. Lett.* **98**, 040403 (2007).
- [9] Zheng Chao, Liang Hao, and Gui Lu Long, *Phil Trans R Soc A*. **371**, 20120053 (2013).
- [10] L. Xiao *et al.*, *Nature Physics*. **13**, 1117-1123 (2017).
- [11] Jian-Shun Tang *et al.*, *Nat. Photon.* **10**, 642-646 (2016).
- [12] Jiaming Li *et al.*, *Nature Communications* **10**, 855 (2019).
- [13] Yang Wu *et al.*, *Science*. **364**, 878 (2019).
- [14] M. Naghiloo, M. Abbasi, Yogesh N. Joglekar, and K. W. Murch, *arXiv*. **1901**, 07968 (2019).
- [15] Kohei Kawabata, Yuto Ashida, and Masahito Ueda, *Phys. Rev. Lett.* **119**, 190401 (2017).
- [16] Yi-Chan Lee, Min-Hsiu Hsieh, Steven T. Flammia, and Ray-Kuang Lee, *Phys. Rev. Lett.* **112**, 130404 (2014).
- [17] Shin-Liang Chen Guang-Yin Chen, and Yueh-Nan Chen, *Phys. Rev. A*. **90**, 054301 (2014).
- [18] Tony E. Lee, Florentin Reiter, and Nimrod Moiseyev, *Phys. Rev. Lett.* **113**, 250401 (2014).
- [19] Romain Couvreur, Jesper Lykke Jacobsen, and Hubert Saleur, *Phys. Rev. Lett.* **119**, 040601 (2017).
- [20] Carl M. Bender, Dorje C. Brody, and Hugh F. Jones, *Phys. Rev. Lett.* **89**, 270401 (2002).
- [21] Carl M. Bender *et al.*, *Phys. Rev. Lett.* **104**, 061601 (2010).
- [22] Kohei Kawabata, Yuto Ashida, and Masahito Ueda, *Phys. Rev. Lett.* **119**, 190401 (2017).
- [23] Sagnik Chakraborty and Dariusz Chruściński, *Phys. Rev. A*. **99**, 042105 (2019).
- [24] S. Haseli *et al.*, *Phys. Rev. A*. **90**, 052118 (2014).
- [25] C. H. Bennett *et al.*, *Phys. Rev. Lett.* **76**, 722 (1996).
- [26] C. H. Bennett, H. J. Bernstein, S. Popescu, and B. Schumacher, *Phys. Rev. A*. **53**, 2046 (1996).
- [27] Heinz-Peter Breuer, Elsi-Mari Laine, Jyrki Piilo, and Bassano Vacchini, *Rev. Mod. Phys.* **88**, 021002 (2016).
- [28] Ángel Rivas, Susana F. Huelga, and Martin B. Plenio, *Phys. Rev. Lett.* **105**, 050403 (2010).
- [29] Peng Peng, Wanxia Cao, Ce Shen, Weizhi Qu, Jianming Wen, Liang Jiang, and Yanhong Xiao, *Nature Physics*. **12**, 1139-1145 (2016).
- [30] You-Lin Chuang, Ziauddin, and Ray-Kuang Lee, *Optics Express*. **18**, 21969-21978 (2018).
- [31] Xin Wang and Jin-Hui Wu, *Optics Express*. **24**, 4289-4298 (2016).
- [32] Li Ge and Hakan E. Türeci, *Phys. Rev. A*. **88**, 053810 (2013).
- [33] Qiang Li *et al.*, *Optica*. **6**, 67-71 (2019).
- [34] Fan Yang, Yong-Chun Liu, and Li You, *Phys. Rev. A*. **96**, 053845 (2017).
- [35] Vladimir V. Konotop and Dmitry A. Zezyulin, *Phys. Rev. Lett.* **120**, 123902 (2018).
- [36] Shaolin Ke, Dong Zhao, Jianxun Liu, Qingjie Liu, Qing Liao, Bing Wang, and Peixiang Lu, *Opt. Express*. **27**, 13858-13870 (2019).
- [37] Xu-Lin Zhang, Tianshu Jiang, Hong-Bo Sun, and C. T. Chan, *arXiv*. **1806**, 07649 (2018).
- [38] Youngsun Choi, Choloong Hahn, Jae Woong Yoon, and Seok Ho Song, *Nature Communications*. **9**, 2182 (2018).
- [39] Li Y *et al.*, *Science* **364**, 170-173, (2019).
- [40] G. L. Long, *Commun. Theor. Phys*. **45**, 825 (2006).
- [41] Guang Hao Low and Isaac L. Chuang, *arXiv*. **1610**, 06546 (2017).
- [42] Guang Hao Low and Isaac L. Chuang, *Phys. Rev. Lett.* **118**, 010501 (2017).
- [43] Chao Zheng, *Europhysics Letters*. **126**, 30005 (2019).
- [44] Dorje C. Brody and Eva-Maria Graefe, *Phys. Rev. Lett.* **109**, 230405 (2012).
- [45] David G. Cory, Amr F. Fahmy, and Timothy F. Havel, *Proc. Natl. Acad. Sci. U.S.A.* **94**, 1634-1639 (1997).
- [46] Shiyao Hou, Yubo Sheng, Guanru Feng, and Guilu Long, *Scientific Reports*. **4**, 6857 (2014).
- [47] Navin Khaneja *et al.*, *Journal of Magnetic Resonance*. **172**, 296 (2005).
- [48] J. S. Lee, *Phys. Rev. A*. **305**, 349 (2002).
- [49] G. M. Leskowitz and L. J. Mueller, *Phys. Rev. A*. **69**, 052302 (2004).
- [50] Jun Li, Shilin Huang, Zhihuang Luo, Keren Li, Dawei Lu, and Bei Zeng, *Phys. Rev. A*. **96**, 032307 (2017).
- [51] Fortunato, E., M. Pravia, N. Boulant, G. Teklemariam, T. Havel, and D. Cory, *J. Chem. Phys.* **116**, 7599 (2002).